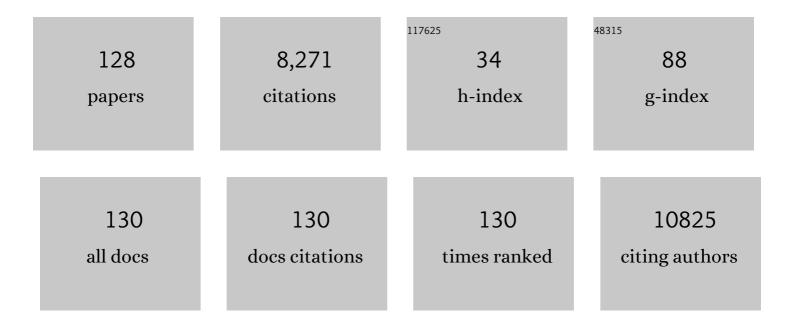
List of Publications by Year in descending order

Source: https://exaly.com/author-pdf/5032448/publications.pdf Version: 2024-02-01



ΚΛΙ ΖΗΛΝΟ

#	Article	IF	CITATIONS
1	Utilizing tannic acid and polypyrrle to induce reconstruction to optimize the activity of MOF-derived electrocatalyst for water oxidation in seawater. Chemical Engineering Journal, 2022, 430, 132632.	12.7	15
2	A strategy combining 3D-DNA Walker and CRISPR-Cas12a trans-cleavage activity applied to MXene based electrochemiluminescent sensor for SARS-CoV-2 RdRp gene detection. Talanta, 2022, 236, 122868.	5.5	59
3	A Dual Photoelectrode Photoassisted Fe–Air Battery: The Photoâ€Electrocatalysis Mechanism Accounting for the Improved Oxygen Evolution Reaction and Oxygen Reduction Reaction of Air Electrodes. Small, 2022, 18, e2103933.	10.0	18
4	Inverted perovskite/silicon V-shaped tandem solar cells with 27.6% efficiency <i>via</i> self-assembled monolayer-modified nickel oxide layer. Journal of Materials Chemistry A, 2022, 10, 7251-7262.	10.3	24
5	Activatable "Matryoshka―nanosystem delivery NgBR siRNA and control drug release for stepwise therapy and evaluate drug resistance cancer. Materials Today Bio, 2022, 14, 100245.	5.5	4
6	Current dilemma in photocatalytic CO2 reduction: real solar fuel production or false positive outcomings?. , 2022, 1, 1.		12
7	What Role Does the Incident Light Intensity Play in Photocatalytic Conversion of CO <sub>2</sub> : Attenuation or Intensification?. ChemPhysChem, 2022, 23, e202100851.	2.1	4
8	In Situ Assembly of MoS <i><sub>x</sub></i> Thinâ€Film through Selfâ€Reduction on p‣i for Drastic Enhancement of Photoelectrochemical Hydrogen Evolution. Advanced Functional Materials, 2021, 31, 2007071.	14.9	22
9	Nickel doping as an effective strategy to promote separation of photogenerated charge carriers for efficient solar-fuel production. Catalysis Science and Technology, 2021, 11, 4012-4015.	4.1	8
10	Experimental Study of the Effect of the Expansion Segment Geometry on the Atomization of a Plain-Jet Airblast Atomizer. International Journal of Aerospace Engineering, 2021, 2021, 1-15.	0.9	2
11	Solarâ€Enhanced CO <sub>2</sub> Conversion with CH <sub>4</sub> over Synergetic NiCo Alloy Catalysts with Lightâ€toâ€Fuel Efficiency of 33.8%. Solar Rrl, 2021, 5, 2100185.	5.8	31
12	Metformin Carbon Dots for Promoting Periodontal Bone Regeneration via Activation of ERK/AMPK Pathway. Advanced Healthcare Materials, 2021, 10, e2100196.	7.6	32
13	Highly Selective Production of Ethanol Over Hierarchical Bi@Bi <sub>2</sub> MoO <sub>6</sub> Composite via Bicarbonateâ€Assisted Photocatalytic CO <sub>2</sub> Reduction. ChemSusChem, 2021, 14, 3293-3302.	6.8	24
14	Solarâ€Enhanced CO <sub>2</sub> Conversion with CH <sub>4</sub> over Synergetic NiCo Alloy Catalysts with Lightâ€toâ€Fuel Efficiency of 33.8%. Solar Rrl, 2021, 5, 2170085.	5.8	3
15	La,Al-Codoped SrTiO <sub>3</sub> as a Photocatalyst in Overall Water Splitting: Significant Surface Engineering Effects on Defect Engineering. ACS Catalysis, 2021, 11, 11429-11439.	11.2	83
16	Construction of hollow polydopamine nanoparticle based drug sustainable release system and its application in bone regeneration. International Journal of Oral Science, 2021, 13, 27.	8.6	15
17	Modification of Metal-Organic Framework Nanoparticles Using Dental Pulp Mesenchymal Stem Cell Membranes to Target Oral Squamous Cell Carcinoma. Journal of Colloid and Interface Science, 2021, 601, 650-660.	9.4	19
18	Hollow mesoporous carbon nanocages with Fe isolated single atomic site derived from a MOF/polymer for highly efficient electrocatalytic oxygen reduction. Journal of Materials Chemistry A, 2021, 9, 22095-22101.	10.3	32

#	Article	IF	CITATIONS
19	The effect of Fe( <scp>iii</scp> ) ions on oxygen-vacancy-rich BiVO <sub>4</sub> on the photocatalytic oxygen evolution reaction. Catalysis Science and Technology, 2021, 11, 7598-7607.	4.1	7
20	Deep-Blue Room-Temperature Phosphorescent Carbon Dots/Silica Microparticles from a Single Raw Material. Langmuir, 2021, 37, 13187-13193.	3.5	19
21	Enabling Molecular Gapping and Bridging on a Biosensing Surface via Electrochemical Cross-Linking and Cleavage. Analytical Chemistry, 2020, 92, 2635-2641.	6.5	2
22	Ascorbic Acid-PEI Carbon Dots with Osteogenic Effects as miR-2861 Carriers to Effectively Enhance Bone Regeneration. ACS Applied Materials & Interfaces, 2020, 12, 50287-50302.	8.0	40
23	Carbon Dots Induce Epithelialâ€Mesenchymal Transition for Promoting Cutaneous Wound Healing via Activation of TGFâ€Î²/p38/Snail Pathway. Advanced Functional Materials, 2020, 30, 2004886.	14.9	19
24	Deep Red Emissive Carbonized Polymer Dots with Unprecedented Narrow Full Width at Half Maximum. Advanced Materials, 2020, 32, e1906641.	21.0	271
25	Selective Growth of Stacking Fault Free ⟠100⟩ Nanowires on a Polycrystalline Substrate for Energy Conversion Application. ACS Applied Materials & Interfaces, 2020, 12, 17676-17685.	8.0	8
26	The preparation of hollow Fe3O4/Pd@C NCs to stabilize subminiature Pd nanoparticles for the reduction of 4-nitrophenol. New Journal of Chemistry, 2020, 44, 4869-4876.	2.8	7
27	Boosting Photocatalytic Oxygen Evolution: Purposely Constructing Direct Z-Scheme Photoanode by Modulating the Interface Electric Field. Chemical Research in Chinese Universities, 2020, 36, 1059-1067.	2.6	22
28	Utilizing in-situ polymerization of pyrrole to fabricate composited hollow nanospindles for boosting oxygen evolution reaction. Applied Catalysis B: Environmental, 2020, 274, 119112.	20.2	23
29	In situ imaging and interfering Dicer-mediated cleavage process via a versatile molecular beacon probe. Analytica Chimica Acta, 2019, 1079, 146-152.	5.4	5
30	Sulfidization of Platinum Nickel Bimetal-Decorated g-C <sub>3</sub> N <sub>4</sub> for Photocatalytic Hydrogen Production: Photogenerated Charge Behavior Study. ACS Sustainable Chemistry and Engineering, 2019, 7, 15137-15145.	6.7	45
31	Facile Synthesis of ZnO-Au Nanopetals and Their Application for Biomolecule Determinations. Chemical Research in Chinese Universities, 2019, 35, 924-928.	2.6	5
32	Ultrasensitive detection of transcription factors with a highly-efficient diaminoterephthalate fluorophore <i>via</i> an electrogenerated chemiluminescence strategy. Chemical Communications, 2019, 55, 11892-11895.	4.1	12
33	Peptide-Based Biosensing of Redox-Active Protein–Heme Complexes Indicates Novel Mechanism for Tumor Survival under Oxidative Stress. ACS Sensors, 2019, 4, 2671-2678.	7.8	5
34	Platelet-driven formation of interface peptide nano-network biosensor enabling a non-invasive means for early detection of Alzheimer's disease. Biosensors and Bioelectronics, 2019, 145, 111701.	10.1	19
35	RNA chaperone assisted intramolecular annealing reaction towards oligouridylated RNA detection in cancer cells. Analyst, The, 2019, 144, 186-190.	3.5	0
36	Hierarchical Hollow Nanocages Derived from Polymer/Cobalt Complexes for Electrochemical Overall Water Splitting. ACS Sustainable Chemistry and Engineering, 2019, 7, 10912-10919.	6.7	31

#	Article	IF	CITATIONS
37	One-step preparation of silica microspheres with super-stable ultralong room temperature phosphorescence. Journal of Materials Chemistry C, 2019, 7, 8680-8687.	5.5	40
38	Remaining Useful Life Prediction of Lithium-Ion Batteries Using Neural Network and Bat-Based Particle Filter. IEEE Access, 2019, 7, 54843-54854.	4.2	83
39	Hole Transfer Channel of Ferrihydrite Designed between Ti–Fe <sub>2</sub> O <sub>3</sub> and CoPi as an Efficient and Durable Photoanode. ACS Sustainable Chemistry and Engineering, 2019, 7, 10971-10978.	6.7	71
40	DNA Tetrahedron Based Biosensor for Argonaute2 Assay in Single Cells and Human Immunodeficiency Virus Type-1 Related Ribonuclease H Detection in Vitro. Analytical Chemistry, 2019, 91, 7086-7096.	6.5	30
41	Ultrasensitive detection of hERG potassium channel in single-cell with photocleavable and entropy-driven reactions by using an electrochemical biosensor. Biosensors and Bioelectronics, 2019, 132, 310-318.	10.1	15
42	Ordered Hybrid Micro/Nanostructures and Their Optical Applications. Advanced Optical Materials, 2019, 7, 1800980.	7.3	22
43	Determination of the activity of uracil-DNA glycosylase by using two-tailed reverse transcription PCR and gold nanoparticle-mediated silver nanocluster fluorescence: a new method for gene therapy-related enzyme detection. Mikrochimica Acta, 2019, 186, 181.	5.0	8
44	Carbonized polymer dots/TiO <sub>2</sub> photonic crystal heterostructures with enhanced light harvesting and charge separation for efficient and stable photocatalysis. Materials Chemistry Frontiers, 2019, 3, 2659-2667.	5.9	16
45	Bone formation promoted by bone morphogenetic protein-2 plasmid-loaded porous silica nanoparticles with the involvement of autophagy. Nanoscale, 2019, 11, 21953-21963.	5.6	15
46	An injectable and thermosensitive hydrogel: Promoting periodontal regeneration by controlled-release of aspirin and erythropoietin. Acta Biomaterialia, 2019, 86, 235-246.	8.3	170
47	Visualized Detection of Polyelectrolytes via 1D Photonic Crystals. Advanced Materials Interfaces, 2019, 6, 1801433.	3.7	5
48	Codelivery of doxorubicin and MDR1-siRNA by mesoporous silica nanoparticles-polymerpolyethylenimine to improve oral squamous carcinoma treatment. International Journal of Nanomedicine, 2018, Volume 13, 187-198.	6.7	49
49	Oneâ€Step Hydrothermal Synthesis of Nitrogenâ€Doped Conjugated Carbonized Polymer Dots with 31% Efficient Red Emission for In Vivo Imaging. Small, 2018, 14, e1703919.	10.0	317
50	Fluorescence Manipulation of Carbon Dots by 1D Photonic Crystals. Advanced Optical Materials, 2018, 6, 1701262.	7.3	10
51	Interleukinâ€6 contributes to chemoresistance in MDAâ€MBâ€231 cells via targeting HIFâ€1α. Journal of Biochemical and Molecular Toxicology, 2018, 32, e22039.	3.0	40
52	Triggering p53 activation is essential in ziyuglycoside lâ€induced human retinoblastoma WERIâ€Rbâ€1 cell apoptosis. Journal of Biochemical and Molecular Toxicology, 2018, 32, e22001.	3.0	10
53	A Sunlight Powered Portable Photoelectrochemical Biosensor Based on a Potentiometric Resolve Ratiometric Principle. Analytical Chemistry, 2018, 90, 13207-13211.	6.5	49
54	Hollow Polypyrrole Nanospindles for Highly Effective Cancer Therapy. ChemPlusChem, 2018, 83, 1127-1134.	2.8	11

#	Article	IF	CITATIONS
55	A sensitive RNA chaperone assay using induced RNA annealing by duplex specific nuclease for amplification. Analytica Chimica Acta, 2018, 1033, 199-204.	5.4	Ο
56	Sensitive detection of cytokine in complex biological samples by using MB track mediated DNA walker and nicking enzyme assisted signal amplification method combined biosensor. Talanta, 2018, 189, 122-128.	5.5	18
57	Polyphyllin I Induces Cell Cycle Arrest and Cell Apoptosis in Human Retinoblastoma Y-79 Cells through Targeting p53. Anti-Cancer Agents in Medicinal Chemistry, 2018, 18, 875-881.	1.7	16
58	Design and synthesis of dodecahedral carbon nanocages incorporated with Fe <sub>3</sub> O <sub>4</sub> . RSC Advances, 2017, 7, 13257-13262.	3.6	10
59	One-step hydrothermal synthesis of photoluminescent carbon nanodots with selective antibacterial activity against Porphyromonas gingivalis. Nanoscale, 2017, 9, 7135-7142.	5.6	201
60	Ultrasensitive fluorescence detection of transcription factors based on kisscomplex formation and the T7 RNA polymerase amplification method. Chemical Communications, 2017, 53, 5846-5849.	4.1	18
61	Puerarin inhibits amyloid β-induced NLRP3 inflammasome activation in retinal pigment epithelial cells via suppressing ROS-dependent oxidative and endoplasmic reticulum stresses. Experimental Cell Research, 2017, 357, 335-340.	2.6	56
62	Au nanorods-sensitized 1DPC for visible detection of NIR light. Journal of Materials Chemistry C, 2017, 5, 2942-2950.	5.5	3
63	Graphene quantum dot based "switch-on―nanosensors for intracellular cytokine monitoring. Nanoscale, 2017, 9, 4934-4943.	5.6	37
64	Amyloid β induces NLRP3 inflammasome activation in retinal pigment epithelial cells via NADPH oxidase― and mitochondriaâ€dependent ROS production. Journal of Biochemical and Molecular Toxicology, 2017, 31, e21887.	3.0	53
65	Strategy for the detection of mercury ions by using exonuclease III-aided target recycling. RSC Advances, 2017, 7, 50420-50424.	3.6	12
66	A novel dual-emission QDs/PCDs assembled composite nanoparticle for high sensitive visual detection of Hg <sup>2+</sup> . RSC Advances, 2017, 7, 49330-49336.	3.6	5
67	Chelation Competition Induced Polymerization (CCIP): A Binding Energy Based Strategy for Nonspherical Polymer Nanocontainers' Fabrication. Chemistry of Materials, 2017, 29, 6536-6543.	6.7	25
68	Neuroprotective effect of tetramethylpyrazine against all-trans-retinal toxicity in the differentiated Y-79 cells via upregulation of IRBP expression. Experimental Cell Research, 2017, 359, 120-128.	2.6	12
69	A new method for sensitive detection of microphthalmia-associated transcription factor based on "OFF-state―and "ON-state―equilibrium of a well-designed probe and duplex-specific nuclease signal amplification. Biosensors and Bioelectronics, 2017, 87, 299-304.	10.1	14
70	Sensitive detection of microRNA in complex biological samples by using two stages DSN-assisted target recycling signal amplification method. Biosensors and Bioelectronics, 2017, 87, 358-364.	10.1	78
71	Entropy-driven reactions in living cells for assay let-7a microRNA. Analytica Chimica Acta, 2017, 949, 53-58.	5.4	17
72	Neuroprotective Effect of Puerarin on Glutamate-Induced Cytotoxicity in Differentiated Y-79 Cells via Inhibition of ROS Generation and Ca2+ Influx. International Journal of Molecular Sciences, 2016, 17, 1109.	4.1	20

#	Article	IF	CITATIONS
73	Ziyuglycoside I Inhibits the Proliferation of MDA-MB-231 Breast Carcinoma Cells through Inducing p53-Mediated G2/M Cell Cycle Arrest and Intrinsic/Extrinsic Apoptosis. International Journal of Molecular Sciences, 2016, 17, 1903.	4.1	25
74	Galectin-1 knockdown in carcinoma-associated fibroblasts inhibits migration and invasion of human MDA-MB-231 breast cancer cells by modulating MMP-9 expression. Acta Biochimica Et Biophysica Sinica, 2016, 48, 462-467.	2.0	32
75	Multifunctional Reversible Fluorescent Controller Based on a One-Dimensional Photonic Crystal. ACS Applied Materials & Interfaces, 2016, 8, 28844-28852.	8.0	14
76	Puerarin Protects Human Neuroblastoma SH‣Y5Y Cells against Glutamateâ€Induced Oxidative Stress and Mitochondrial Dysfunction. Journal of Biochemical and Molecular Toxicology, 2016, 30, 22-28.	3.0	25
77	FoxM1 inhibition enhances chemosensitivity of docetaxel-resistant A549 cells to docetaxel via activation of JNK/mitochondrial pathway. Acta Biochimica Et Biophysica Sinica, 2016, 48, 804-809.	2.0	26
78	Highly efficient aqueous-processed polymer/nanocrystal hybrid solar cells with an aqueous-processed TiO <sub>2</sub> electron extraction layer. Journal of Materials Chemistry A, 2016, 4, 11738-11746.	10.3	26
79	Induction of oxidative and nitrosative stresses in human retinal pigment epithelial cells by all-trans-retinal. Experimental Cell Research, 2016, 348, 87-94.	2.6	24
80	Chelation competition induced polymerization (CCIP): construction of integrated hollow polydopamine nanocontainers with tailorable functionalities. Chemical Communications, 2016, 52, 10155-10158.	4.1	36
81	Aspirin-Based Carbon Dots, a Good Biocompatibility of Material Applied for Bioimaging and Anti-Inflammation. ACS Applied Materials & Interfaces, 2016, 8, 32706-32716.	8.0	140
82	A label-free kissing complex-induced fluorescence sensor for DNA and RNA detection by using DNA-templated silver nanoclusters as a signal transducer. RSC Advances, 2016, 6, 99269-99273.	3.6	6
83	Effective delivery of bone morphogenetic protein 2 gene using chitosan–polyethylenimine nanoparticle to promote bone formation. RSC Advances, 2016, 6, 34081-34089.	3.6	18
84	A label-free kissing complexes-induced fluorescence aptasensor using DNA-templated silver nanoclusters as a signal transducer. Biosensors and Bioelectronics, 2016, 78, 154-159.	10.1	28
85	Electrophoretic deposition of fluorescent Cu and Au sheets for light-emitting diodes. Nanoscale, 2016, 8, 395-402.	5.6	21
86	Sensitive detection of transcription factors in cell nuclear extracts by using a molecular beacons based amplification strategy. Biosensors and Bioelectronics, 2016, 77, 264-269.	10.1	26
87	Gas1 Knockdown Increases the Neuroprotective Effect of Glial Cell-Derived Neurotrophic Factor Against Glutamate-Induced Cell Injury in Human SH-SY5Y Neuroblastoma Cells. Cellular and Molecular Neurobiology, 2016, 36, 603-611.	3.3	9
88	Tetramethylpyrazine Protects Retinal Capillary Endothelial Cells (TR-iBRB2) against IL-1β-Induced Nitrative/Oxidative Stress. International Journal of Molecular Sciences, 2015, 16, 21775-21790.	4.1	26
89	Heterostructures: Au-Edged CuZnSe2Heterostructured Nanosheets with Enhanced Electrochemical Performance (Small 29/2015). Small, 2015, 11, 3582-3582.	10.0	0
90	Surface Ligand Dynamics-Guided Preparation of Quantum Dots–Cellulose Composites for Light-Emitting Diodes. ACS Applied Materials & Interfaces, 2015, 7, 15830-15839.	8.0	57

#	Article	IF	CITATIONS
91	Investigating the surface state of graphene quantum dots. Nanoscale, 2015, 7, 7927-7933.	5.6	196
92	Au-Edged CuZnSe2Heterostructured Nanosheets with Enhanced Electrochemical Performance. Small, 2015, 11, 3583-3590.	10.0	8
93	Photoluminescent graphene quantum dots for in vitro and in vivo bioimaging using long wavelength emission. RSC Advances, 2015, 5, 39399-39403.	3.6	42
94	Assembly-Induced Enhancement of Cu Nanoclusters Luminescence with Mechanochromic Property. Journal of the American Chemical Society, 2015, 137, 12906-12913.	13.7	367
95	A new signal-on method for the detection of protein based on binding-induced strategy and photoinduced electron transfer between Ag nanoclusters and split G-quadruplex-hemin complexes. Analytica Chimica Acta, 2015, 887, 224-229.	5.4	11
96	Sensitive and selective amplified detection of silver ion based on NEase-aided target recycling. RSC Advances, 2015, 5, 89047-89051.	3.6	4
97	Binding-induced and label-free colorimetric method for protein detection based on autonomous assembly of hemin/G-quadruplex DNAzyme amplification strategy. Biosensors and Bioelectronics, 2015, 64, 572-578.	10.1	52
98	Sustained release poly (lactic-co-glycolic acid) microspheres of bone morphogenetic protein 2 plasmid/calcium phosphate to promote in vitro bone formation and in vivo ectopic osteogenesis. American Journal of Translational Research (discontinued), 2015, 7, 2561-72.	0.0	8
99	Efficiently engineered cell sheet using a complex of polyethylenimine–alginate nanocomposites plus bone morphogenetic protein 2 gene to promote new bone formation. International Journal of Nanomedicine, 2014, 9, 2179.	6.7	19
100	Rational design of signal-on biosensors by using photoinduced electron transfer between Ag nanoclusters and split G-quadruplex halves–hemin complexes. Chemical Communications, 2014, 50, 14221-14224.	4.1	35
101	High level soluble expression, purification, and characterization of human ciliary neuronotrophic factor in Escherichia coli by single protein production system. Protein Expression and Purification, 2014, 96, 8-13.	1.3	4
102	Sensitive and selective amplified visual detection of cytokines based on exonuclease III-aided target recycling. Chemical Communications, 2014, 50, 13342-13345.	4.1	29
103	Facile fabrication of mesoporous N-doped Fe <sub>3</sub> O <sub>4</sub> @C nanospheres as superior anodes for Li-ion batteries. RSC Advances, 2014, 4, 713-716.	3.6	15
104	Label-free and ultrasensitive fluorescence detection of cocaine based on a strategy that utilizes DNA-templated silver nanoclusters and the nicking endonuclease-assisted signal amplification method. Chemical Communications, 2014, 50, 180-182.	4.1	61
105	Characteristics of three sizes of silica nanoparticles in the osteoblastic cell line, MC3T3-E1. RSC Advances, 2014, 4, 46481-46487.	3.6	11
106	Ziyuglycoside II induces cell cycle arrest and apoptosis through activation of ROS/JNK pathway in human breast cancer cells. Toxicology Letters, 2014, 227, 65-73.	0.8	62
107	Ultrasensitive detection of microRNA with isothermal amplification and a time-resolved fluorescence sensor. Biosensors and Bioelectronics, 2014, 57, 91-95.	10.1	35
108	DNA-templated silver nanoclusters based label-free fluorescent molecular beacon for the detection of adenosine deaminase. Biosensors and Bioelectronics, 2014, 52, 124-128.	10.1	36

#	Article	IF	CITATIONS
109	The effect of puerarin against IL-1Î <sup>2</sup> -mediated leukostasis and apoptosis in retinal capillary endothelial cells (TR-iBRB2). Molecular Vision, 2014, 20, 1815-23.	1.1	25
110	A new method for the detection of adenosine based on time-resolved fluorescence sensor. Biosensors and Bioelectronics, 2013, 49, 226-230.	10.1	14
111	An enzyme substrate binding aptamer complex based time-resolved fluorescence sensor for the adenosine deaminasedetection. Biosensors and Bioelectronics, 2013, 42, 87-92.	10.1	19
112	Highly Photoluminescent Carbon Dots for Multicolor Patterning, Sensors, and Bioimaging. Angewandte Chemie - International Edition, 2013, 52, 3953-3957.	13.8	2,907
113	Facile synthesis of manganese oxide loaded hollow silica particles and their application for methylene blue degradation. Journal of Colloid and Interface Science, 2013, 405, 28-34.	9.4	22
114	A new strategy based on aptasensor to time-resolved fluorescence assay for adenosine deaminase activity. Biosensors and Bioelectronics, 2013, 41, 123-128.	10.1	20
115	A facile two-step etching method to fabricate porous hollow silica particles. Journal of Colloid and Interface Science, 2012, 384, 22-28.	9.4	35
116	Establishment and Validation of a Time-Resolved Fluoroimmunoassay for Chlorpromazine. Food Analytical Methods, 2012, 5, 625-630.	2.6	14
117	Synthesis and Assembly of Core/Shell Nanospheres. Journal of Nanoscience and Nanotechnology, 2009, 9, 7428-31.	0.9	2
118	A Universal Approach to Fabricate Various Nanoring Arrays Based on a Colloidalâ€Crystalâ€Assistedâ€Lithography Strategy. Advanced Functional Materials, 2008, 18, 4036-4042.	14.9	64
119	Inside Front Cover: A Universal Approach to Fabricate Various Nanoring Arrays Based on a Colloidal-Crystal-Assisted-Lithography Strategy (Adv. Funct. Mater. 24/2008). Advanced Functional Materials, 2008, 18, NA-NA.	14.9	0
120	Preparation of fluorescent poly(methylmethacrylate) nano capsules via internal phase separation. E-Polymers, 2007, 7, .	3.0	2
121	Synthesis and characterization of novel star polymer with β-cyclodextrin core and its metal complexes. Journal of Applied Polymer Science, 2007, 106, 28-33.	2.6	5
122	Synthesis and characterization of polymer brushes containing metal nanoparticles. Polymer Bulletin, 2006, 57, 253-259.	3.3	9
123	Synthesis and properties of novel macromolecular coupling agents prepared by ATRP. Journal of Applied Polymer Science, 2006, 102, 3919-3926.	2.6	6
124	Synthesis and properties of novel end-functionalized polybutylacrylate and its metal complexes. Polymer Bulletin, 2005, 55, 447-456.	3.3	3
125	Two-substrate vertical deposition for stable colloidal crystal chips. Science Bulletin, 2005, 50, 765-769.	1.7	1
126	Hollow Titania Spheres with Movable Silica Spheres Inside. Langmuir, 2004, 20, 11312-11314.	3.5	125

#	Article	IF	CITATIONS
127	Monodisperse Silica-Polymer Core-Shell Microspheres via Surface Grafting and Emulsion Polymerization. Macromolecular Materials and Engineering, 2003, 288, 380-385.	3.6	187
128	A novel method for the layer-by-layer assembly of metal nanoparticles transported by polymer microspheres. Journal of Materials Chemistry, 2003, 13, 514-517.	6.7	35